Al-Rafidain Engineering Journal (AREJ) Vol.31, No.1, March 2026, pp. 34-48

Thermal Performance Enhancement of Solar Air Heaters Using Multi-V-Shaped Perforated Ribs With Different Directions

Alind Ghasan Salih* ✉**Omar Mohammed Hamdoon****
alend.salih@visitor.uoz.edu.krd eng.omar.m.hamdoon@uomosul.edu.iq

* Mechanical Engineering Department, College of Engineering, University of Zakho, Zakho, Iraq
* Engineering Research Center, University of Zakho, Zakho, Iraq
** Mechanical Engineering Department, College of Engineering, University of Mosul, Mosul, Iraq

Received: June 22th 2025 Received in revised form: September 26th 2025 Accepted: December 3rd 2025

ABSTRACT

This experimental study investigates the thermal performance of three solar air heater (SAH) configurations: a conventional flat plate, a V-up perforated ribs absorber plate, and a V-down perforated ribs absorber plate. The studies were conducted in real outdoor conditions at the University of Zakho, Zakho, Iraq, on 15, 18, and 25 February 2025. Each SAH was tested at three different air mass flow rates: 0.00882 kg/s, 0.01323 kg/s, and 0.01764 kg/s. The findings demonstrated that the V-down SAH consistently outperformed the others in terms of daily thermal efficiency and heat gain. At the maximum flow rate (0.01764 kg/s), the V-down configuration achieved a maximum daily thermal efficiency of 84% and a peak useful heat transfer rate of 529 W. The V-up SAH followed with 77% efficiency and 492 W, while the flat plate SAH reached 69% efficiency and 470 W. The enhanced performance of the V-down design is attributed to improved turbulence and convective heat transfer induced by its downward-facing perforated ribs. These findings confirm the effectiveness of using V-shaped perforated ribs, particularly the V-down orientation, in enhancing the thermal performance of solar air heaters.

Keywords:

Solar air heater, V-shaped perforated ribs, thermal efficiency, airflow rate, useful heat gain.

This is an open access article under the CC BY 4.0 license (http://creativecommons.org/licenses/by/4.0/).
https://jamh.uomosul.edu.iq/index.php/arej/index
Email: alrafidain_engjournal3@uomosul.edu.iq

==========

1. INTRODUCTION

Environmental pollution and diseases that threaten human health are linked to the consumption of fossil fuel energy sources. The rise in human population has been accompanied by increased energy requirements, economic and technological development, industrialization, and a global surge in energy demand. Consequently, researchers have focused on renewable energy sources. Solar energy is a crucial renewable resource due to the relatively low costs associated with solar technologies and their environmentally friendly nature [1].

The solar air heater is a device that converts solar radiation into thermal energy to heat air. Solar air heaters are among the most popular devices designed for solar energy capture, due to their simplicity, low cost, and low maintenance requirements. The SAH consists of a glass cover, an absorber plate, an airflow path, and insulation to reduce heat losses from the bottom and side walls of the solar collector. A blower or fan is used to supply air to the heater channel. Hot air from SAH, maintained at temperatures below 100°C, is employed for agricultural product drying (spices, fruits, vegetables, and herbs) and space heating of residential and commercial buildings [2].

The efficiency of a conventional flat plate solar air heater is generally limited due to the low heat transfer coefficient between the absorber plate and the circulating air, resulting in elevated temperatures of the absorber plate and increased heat loss [3]. The efficiency of a conventional flat plate solar air heater (SAH) can be improved by introducing artificial roughness on the absorber plate surface. Adding repeated ribs to the surface can significantly enhance heat transfer from the absorber plate to the air by altering the airflow. Repeated ribs modify the flow field, improve the flow turbulence, and increase substantially the heat transfer coefficient [4].

Numerous studies have examined the impact of varying geometries and configurations of

artificial roughness on the enhancement of heat transfer in solar air heaters.

Momin et al. [5] conducted an experimental study to examine how V-shaped ribs affect heat transfer and friction in a SAH. The experimental study was performed at Reynolds numbers (Re) from 2500 to 18000, relative roughness heights (e/D_h) between 0.02 and 0.034, and angles of attack (α) from 30° to 90°. The findings revealed a substantial improvement in the Nusselt number, exhibiting a maximum increase of 2.30 times relative to smooth ducts, alongside a friction factor escalation of 2.83 times at an optimal angle of 60°.

Hans et al. [6] performed an experimental study to investigate the influence of multiple v-rib roughness on the heat transfer and friction factor in the duct of a SAH. Experiments were carried out at (Re) from 2000 to 20000, (e/D_h) of 0.019 - 0.043, relative roughness pitch (P/e) of 6 - 12, and relative roughness width (W/w) of 1 - 10. The results indicate that the highest increase in heat transfer occurs at (W/w) = 6, and the maximum friction factor occurs at (W/w) = 10. Furthermore, the Nusselt number (Nu) and the friction factor (f) reach their peak values at α = 60°, resulting in a significant increase in heat transfer and pressure drop compared to smooth ducts, by up to 6 and 5 times, respectively.

Singh, Chander, Saini, et al. [7] Executed an experimental investigation to examine the effect of V-down ribs arrangement roughness on heat transfer and friction factor in a rectangular air passage solar air heater duct with (w/b) = 12 . In the experiment, the ribs had a (e/Dh) = 0.043, (α) = 60°, and a (P/e) = 10. The model tests were conducted over a (Re) range of 3000 to 15000. The position of the gaps (g/e) was also one of the parameters varied to determine its influence on thermohydraulic performance, ranging from (g/e) = 0.20 to (g/e) = 0.80. It was observed that a (g/e) of 0.65 was the optimal value, and the correlation increased the (Nu) and (f) by factors of 2.88 and 3.03, respectively, compared to the smooth duct.

Singh, Chander, & Saini. [8] Conducted an experimental study to investigate the impact of discrete V-down rib-roughened SAH on thermal efficiency, demonstrating an increase of up to 91% in effective efficiency relative to traditional flat plate designs. This improvement is due to increased turbulence, although it also results in higher pumping power requirements. The optimal parameters for maximizing effective efficiency are as follows: (P/e) = 8, (g/e) = 1, (d/w) = 0.65, (α) = 60°, and (e/D_h) = 0.043. The research indicates that rib-roughened designs are most effective at Reynolds numbers below 20000, whereas conventional designs demonstrate superior performance at Reynolds numbers exceeding 30500.

Singh, Chander, & Saini. [9] conducted an experimental study to investigate the thermo-hydraulic performance of rectangular ducts with V-down rib roughness featuring a gap. Executed with an (w/b) = 12, the roughness exhibits a (e/D_h) = 0.043 and a (P/e) = 8, with (Re) varying from 3000 to 15000. The study investigated flow-attack angles (α) ranging from 30° to 75°. The measured key parameters included (f), (Nu), and a thermo-hydraulic performance parameter (g) based on equivalent pumping power. The results indicate that the optimal performance parameter (g) is 2.06. It is achieved at (α) = 60° and a (Re) = 12000, indicating enhanced performance relative to smooth ducts.

Karwa & Chitoshiya. [10] carried out an experimental study to investigate the thermo-hydraulic performance of (SAH) featuring rib roughness on the absorber plate, specifically using a V-down discrete rib, compared to a smooth duct air heater. The rib roughness is shown to increase the thermal performance by 12.5% to 20%, in particular, at lower mass flow rates. This study validates a mathematical model using experimental data, enabling the prediction of performance for both smooth and roughened air heaters under various conditions. Airflow rates and thermal performance are the key parameters, indicating a pronounced effect of rib roughness on performance.

Kumar & Saini. conducted an experimental study to analyze the impact of discrete multi-V-shaped rib roughness on the thermo-hydraulic performance characteristics of solar air heaters. The (Re) was varied between 2000 and 20000, and (W/w) was varied from 1 to 10, with all other parameters held constant: relative gap distance (Gd/Lv) = 0.69, (g/e) = 1, (P/e) = 8, (e/D_h) = 0.043, and (α) = 60°. The conclusions indicate that the optimum roughness geometry (W/w = 6 at Re = 20000) significantly enhances the thermal performance.

Singh et al. [11] conducted experimental work on the thermo-hydraulics of V-down ribs with gaps in solar air heater ducts, detailing how variations in relative roughness pitches of 4, 6, 8, 10, and 12 affect the Reynolds number (Re), which was controlled within a range from 3000 to 15,000. The present study simulated a duct with a (w/b) value of 12. A uniform heat flux was applied to a roughened wall surface, and the other three walls were insulated. It is observed that the (f) and (Nu) were maximum for a (P/e) of 8, with the peak values of 2.70 and 2.86, respectively. The (g)

ranged from 1.27 to 1.93, exhibiting increased effectiveness in the ribbed ducts as compared to the smooth ducts. The study indicates that this rib geometry outperforms other designs, particularly for Reynolds numbers ranging from 3000 to 12000. Istanto et al. [12] conducted an experimental study to investigate the enhancement of heat transfer to a solar air heater by using V-down continuous ribs with different angles of attack. An electric furnace was used to model the phenomenon under these conditions, with (Re) from 3500 to 10000. The essential parameters were (W/H) = 12, (P/e) = 10, and (e/D_h) = 0.033. It has been found that the maximum enhancements of (Nu) and (f) were 2.34 and 2.45 times, respectively, compared to a smooth duct. The artificial roughness achieved the best thermo-hydraulic performance at (α) = 60°, and a 37.33% enhancement was achieved using the artificial roughness element for solar air heater performance.

Patel & Lanjewar. [13] carried out an experimental study on thermal enhancement of an SAH duct with staggered elements in a discrete V-rib configuration. It is based on the heat transfer and friction characteristics in a rectangular duct for Reynolds numbers 3000 to 12000. Characteristic parameters include a staggered size-to-rib height ratio (r/e) of 2 - 5.5, (P/e) of 12, (e/D_h) of 0.045, and (α) of 60°. The design is such that for (g/e) of 1, staggered element position (p'/p) of 0.65, and six gaps (Ng), cascaded gaps are formed. The optimal Stanton number of 1.90 and an optimum thermal efficiency of 86% are observed at (r/e)= 3.5. Jain et al. [14] conducted an experimental investigation of the thermal performance of a solar air heater with multi-gap V-roughness and staggered elements using experimental techniques and ANN. The experiments performed in a rectangular channel with a roughened side resulted in an augmentation of maximum thermal efficiency from 42.15% to 87.02% at Re = 3000 - 14000. The optimal values found are P/e = 12 and w/g = 1.

Balakrishnan et al. [15] carried out an experimental study to explore the combined effect of polygonal ribs and phase change material (PCM, paraffin wax) on the thermal performance of a solar air heater (SAH), The results indicated that the ribbed absorber with PCM achieved the best performance, with a peak outlet temperature of 77 °C at 0.062 kg/s and an extended heat release duration of 3.5 h, compared to 2 h for the flat plate with PCM. Without PCM, the polygonal rib plate still outperformed the flat plate, reaching 79°C versus 73°C, due to enhanced turbulence and convective heat transfer. The findings highlight the effectiveness of combining artificial roughness with thermal storage to improve both efficiency and operating duration.

Zubairi et al. [16] conducted an experimental and computational study to investigate dual-flow solar air heaters (SAHs) with flat, trapezoidal, and U-corrugated absorber plates. Experiments in Baghdad, Iraq, during April – May 2022 tested four airflow rates from 0.0011 to 0.0046 kg/s with a 30° south tilt. At the highest flow rate, efficiencies were 43% (flat), 51% (U-corrugated), and 54% (trapezoidal). Anti-parallel airflow further improved the U-corrugated plate efficiency to 55.53%, achieving a maximum energy gain of 199 W. Experimental and simulated results were closely aligned, with only 5.7% deviation. Corrugation, especially U-corrugation with anti-parallel flow, significantly enhanced heat transfer and thermal efficiency.

Rajendran et al. [17] conducted an experimental study to explain the enhancement of SAH efficiency by the use of a broken V-rib on the absorber plate. This work compares a conventional flat absorber plate (FSAH) and a broken V-rib-shaped absorber plate (VSAH) at three air velocities of 25 m/s, 20 m/s, and 15 m/s (which correspond to mass flow rates of 0.037 kg/s, 0.031 kg/s, and 0.023 kg/s, respectively). The results showed that the VSAH yields an enhanced useful power of about 16.6% - 19.8% over the FSAH with a lower maximum absorber temperature of 0.6℃ - 1.4℃. The thermal efficiency of the VSAH has responses compared with the FSAH, namely 20.5 % - 15.7 %.

Although numerous studies have investigated the thermal performance of solar air heaters using artificial roughness, many have been limited to single rib orientations, fixed operating conditions, or theoretical simulations. Several experimental investigations have utilized V-shaped ribs; however, few have directly compared both V-up and V-down perforated ribs under identical environmental conditions and across multiple airflow rates. Moreover, comparative evaluation with a flat plate baseline has often been neglected.

The present study addresses these gaps by experimentally examining three distinct SAH configurations: flat plate, V-down, and V-up perforated absorber plates. While the concept of V-shaped and perforated ribs has been widely reported in the literature, the novelty of this work lies in providing confirmatory validation of their performance under real outdoor conditions in Iraq. By systematically comparing rib orientation, airflow variation, and baseline flat plate performance, this study contributes region-specific

experimental evidence that strengthens and contextualizes previous findings.

2. DATA REDUCTION

In this section, the experimental data were processed to determine the thermal performance of the solar air heater, including mass flow rate, useful heat gain, and thermal efficiency, using standard thermodynamic equations based on measured temperatures, air velocity, and solar radiation.

1. Mass Flow Rate ($\dot{m}$):

The calculation of the air mass flow rate was performed using [18]:

$$\dot{m} = \rho \times A_C \times V \quad (1)$$

Where:

ρ : air density (kg/m^3).

A_C: cross-sectional area of the duct (m^2).

V: a velocity of air at the duct inlet (m/s).

2. Useful Heat Gain (Q_u)

The rate of useful energy gained by the air was determined from [18]:

$$Q_u = \dot{m} \times Cp \times (T_{out} - T_{in}) \quad (2)$$

Where:

Cp : Specific heat of air ($J/kg \times K$),

T_{in} , T_{out}: Inlet and outlet air temperatures (°C).

3. Thermal Efficiency (η_{th})

The thermal efficiency of the SAH was calculated as [19]:

$$\eta_{th} = Q_u / (A_S \times I) \quad (3)$$

Where:

A_S : surface area of the collector (m^2).

I : Solar irradiance incident on the collector surface (W/m^2).

3. EXPERIMENTAL SETUP

The experimental solar air heater system was installed on the rooftop of the Presidency Building at the University of Zakho, Zakho, Iraq. The location is geographically situated at a latitude of 37.15°N and a longitude of 42.68°E. The system was oriented due south and tilted at an angle of 55° to maximize solar radiation capture based on the site's solar path [20]. Figure 1 shows a real photo of the constructed solar air heater (SAH) systems the setup consisted of three identical rectangular

Fig. 1 The real photo of the constructed solar air heater systems.

test ducts (120 × 60 × 12 cm³). Each duct was covered with a 6 mm-thick transparent glass sheet (60 cm × 100 cm), and the duct structure was made from wood. The back and side walls of each duct were insulated using a three-layer system composed of: (1) an outer 18 mm thick film-faced birch plywood layer, (2) a 20 mm thick polystyrene foam layer, and (3) an inner layer of birch plywood. All wooden surfaces were finished with a wood stain varnish to protect against weathering and moisture. Figure 2 shows the schematic cross-section of the duct system.

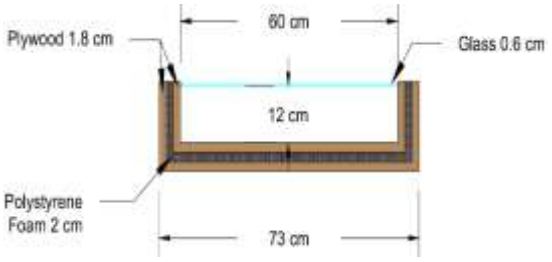

Fig. 2 The schematic cross-section of the duct of the SAH system.

Three absorber plate configurations were tested: a flat plate (reference), V-up perforated ribs, and V-down perforated ribs. All plates were made of 1 mm-thick aluminum and painted matte black to enhance solar absorption. Each ribbed plate contained 14 aluminum ribs mounted on the bottom surface, designed according to optimal roughness parameters reported in previous experimental studies [21]. All ribs had identical geometrical parameters (pitch, height, angle, and hole size), with variation only in their orientation (V-up or V-down). Figure 3 presents a schematic drawing of the absorber plates showing the uniform distribution of ribs. The perforated V-ribs, oriented both upward and downward, promote airflow and enhance heat transfer, allowing for a direct performance comparison between configurations. An overview of the experimental system specifications is provided in Table 1.

Airflow was generated by a centrifugal blower connected to a diffuser. The diffuser was wrapped with foil-backed glass fiber insulation to reduce thermal losses. The blower's speed was regulated using an electronic dimmer to achieve three different mass flow rates: 0.00882 kg/s, 0.01323 kg/s, and 0.01764 kg/s.

Table 1. Geometric Parameters of the Solar Air Heater System

Parameter	Symbol	Value
Length of duct	L	**120 cm**
Width of the duct	W	**60 cm**
Height of the duct	H	**12 cm**
Absorber plate thickness	-	**1 mm**
Number of ribs per duct	-	**14**
Rib height	e	**1.2 cm**
Rib thickness	-	**1 mm**
Rib length	-	**17 cm**
Pitch between ribs	P	**12 cm**
Diameter of perforations	-	**6 mm**
Angle of attack	α	**45°**
Duct aspect ratio	A/R	**5**
Relative roughness height	e/D_h	**0.06**
Relative roughness pitch	P/e	**10**
Relative rib width ratio	W/w	**5**
Hydraulic diameter	D_h	**20 cm**
Collector area	-	**0.6 m²**

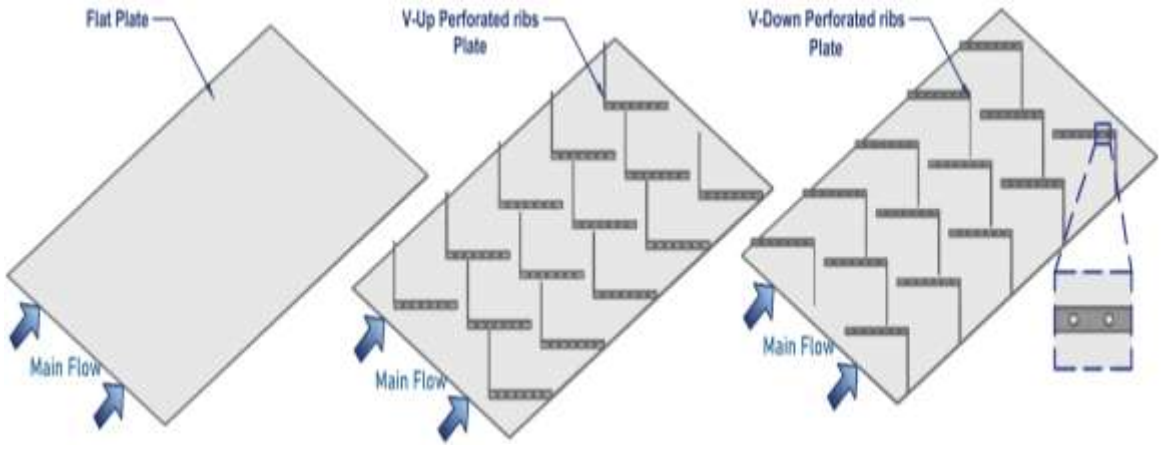

(a) (b) (c)

Fig. 3 A schematic drawing of the absorber plates, (a) flat smooth plate, (b) V-up perforated rib plate and (c) V-down perforated rib plate.

Temperature measurements were recorded using DS18B20 digital temperature sensors with an accuracy of ± 0.5°C. Each duct was equipped with three sensors on the absorber plate and three sensors on the glass cover. Additionally, two sensors were installed at the air inlet and two at the air outlet, and one more sensor measured ambient air temperature. To ensure the accuracy and reliability of the temperature readings, a calibration was performed between the DS18B20 sensors and a standard mercury thermometer, as shown in Figure 4.

Solar radiation was measured using a YGC-JYZ photoelectric total radiation sensor with an accuracy of $\pm$ 5%. The sensor has a resolution of $1\ W/m^2$ and a measuring range of 0 - 1500 W/m². This solar sensor was calibrated to ensure the accuracy of the measurements. It was installed with the same tilt angle of 55° as the solar air heater system to align with the sun's path during testing.

Data logging was performed using an Arduino Uno R3, in combination with a DS1302 RTC module for time tracking and a micro-SD card module for storing recorded data. Hourly data were collected between 9:00 and 16:00 under stable atmospheric conditions, with measurements recorded at 30-minute intervals.

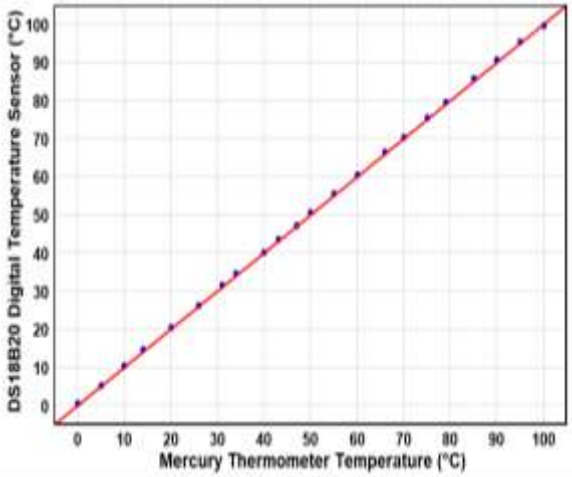

Fig. 4 A calibration between the DS18B20 sensors and a standard mercury thermometer.

4. RESULTS AND DISCUSSIONS

This section presents and discusses the experimental results obtained from testing three different solar air heater (SAH) configurations: flat plate, V-down perforated, and V-up perforated absorber plates. The experiments were conducted on three separate days, 15, 18, and 25 February 2025, under varying solar and ambient conditions. Temperature and solar radiation data were recorded every 30 minutes from 9:00 to 16:00, providing detailed insight into hourly performance trends. Each test was repeated using various air mass flow rates to assess how airflow velocity affects thermal behavior and efficiency across the three configurations. The results are analyzed to evaluate the impact of absorber plate design, airflow rate, and environmental conditions on the thermal performance and daily efficiency of each SAH system. Special emphasis is placed on comparing the effectiveness of the V-shaped perforated ribs (both V-down and V-up) in enhancing heat transfer relative to the conventional flat plate design. These comparisons aim to determine which configuration provides the highest heat gain and under what operating conditions it performs best.

Figure 5 illustrates the variation of solar radiation and ambient temperature on 15, 18, and 25 February 2025. Across all days, solar radiation followed a typical daily pattern, rising from 9:00 AM, peaking between 12:30 and 13:00, and declining in the afternoon as the sun's angle decreased.

On 15 February, the radiation rose from about 520 W/m² to a peak of 1040 W/m^2 at 12:30 PM, then dropped to 700 W/m^2 by 4:00 PM. The sky was mostly clear, resulting in stable radiation. The ambient temperature increased from 6°C to 24°C, closely following the radiation curve.

On 18 February, although solar radiation was slightly lower, starting at 490 W/m² and peaking at 1020 W/m^2, the ambient temperature reached its highest value of about 27°C. This was likely due to calm atmospheric conditions and reduced wind, which minimized heat loss despite possible light cloud cover around midday.

On 25 February, radiation exceeded 1050 W/m^2, the highest among the three days. The clear sky and minimal cloud interference boosted solar input, but the ambient temperature only reached 14.5°C, slightly lower than on 18 February, as light winds cooled the environment.

Figure 6 presents the daily thermal efficiency of the flat plate SAH, V-down SAH, and V-up SAH on 15, 18, and 25 February 2025 under different mass flow rates.

On 15 February ($\dot{m} = 0.01764$ kg/s), all systems achieved their best performance due to the high and steady solar radiation (peak 1040 W/m²) and stable ambient temperature (reaching 21°C). The V-down SAH reached 84%, followed by V-up at 77% and flat SAH at 69%. Strong solar input and reduced heat loss due to warmer ambient air contributed to these high efficiencies.

On 18 February ($\dot{m} = 0.00882$ kg/s), the lowest mass flow rate increased air residence time, but the slightly lower radiation (1020 W/m²)

and possibly intermittent cloud cover around midday reduced overall efficiency. The V-down, V-up, and flat SAHs recorded 43%, 39%, and 36%, respectively. The higher ambient temperature (27°C) helped limit convective losses, but reduced solar gain was the limiting factor.

On 25 February ($\dot{m} = 0.01323$ kg/s), efficiencies were moderate: 56% (V-down), 50% (V-up), and 47% (flat). Although this day had the highest solar radiation (1050 W/m^2), the mass flow rate was neither too high nor too low, creating a balance between effective heat absorption and convective heat extraction. The ambient temperature (14.5°C) and clear skies supported stable thermal behavior. Overall, the downward-facing perforated ribs' enhanced turbulence and improved heat transfer contribute to the V-down SAH's superior performance. The variations across the days underscore the synergistic impact of solar radiation, ambient temperature, and airflow rate on thermal efficiency.

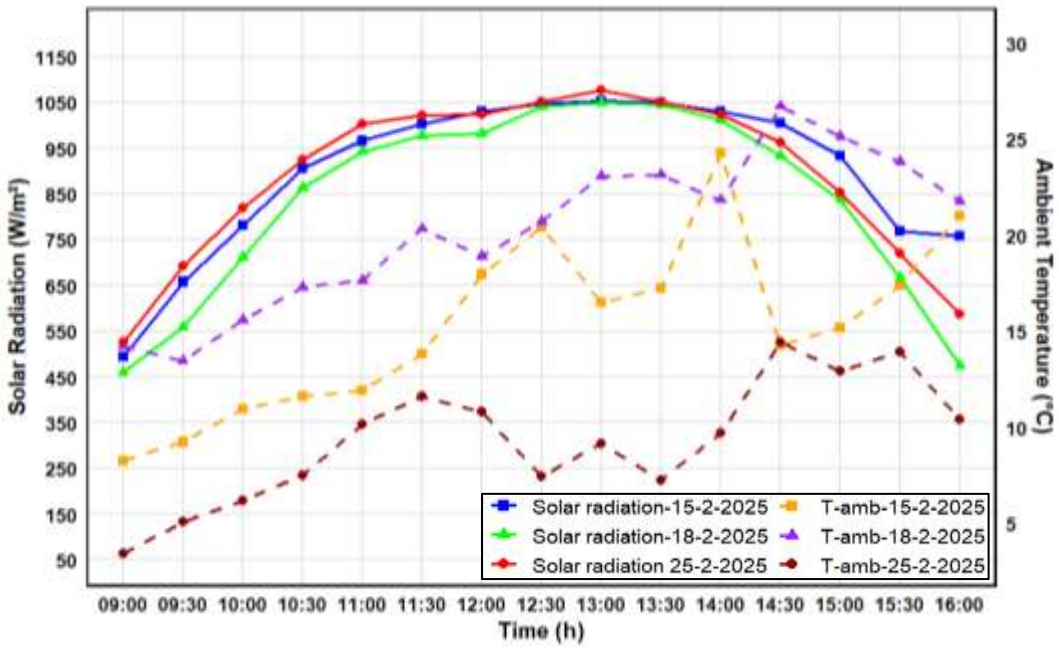

Fig. 5 The variation of solar radiation and ambient temperature on different days in February 2025.

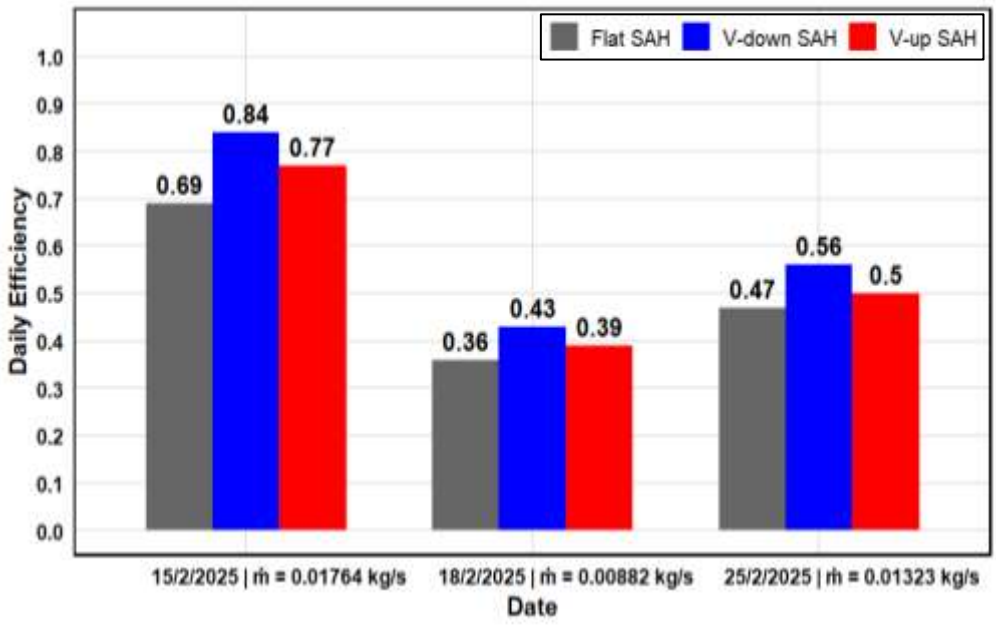

Fig. 6 Comparison of Daily Thermal Efficiency of SAHs on Different Days with Varying Airflow Rates in February 2025.

Figure 7 illustrates the variation of outlet air temperature (T_{out}), absorber plate temperature (T_{plate}), and glass cover temperature (T_{glass}) for the flat, V-down, and V-up SAHs on 15 February 2025, under the highest tested mass flow rate of 0.01764 kg/s.

At the beginning of the experiment (09:00), the outlet temperatures were relatively low due to cooler morning conditions and limited initial solar radiation. The recorded values were 19°C (V-down), 16°C (flat), and 15°C (V-up). As the sun rose higher and solar radiation increased significantly (reaching its peak of around 1040 W/ m^2 at 12:30), the temperatures increased accordingly. Around 13:00, all systems reached their peak outlet air temperatures: 46°C for V-down, 44°C for V-up, and 43°C for flat SAH. The V-down SAH outperformed the others due to the improved turbulence and enhanced air surface contact induced by the downward-facing perforated ribs, which increased convective heat transfer.

Absorber plate temperatures peaked between 13:00 and 13:30, with maximum values of approximately 74 °C (V-down), 73 °C (V-up), and 73 °C (flat). The similarity in Tplate values is due to equal exposure to sunlight, but differences in outlet temperature reflect the varying levels of air mixing and heat extraction. The glass cover temperatures followed a similar trend, peaking at 42°C (V-down) and 41°C for both flat and V-up systems. By 16:00, the outlet temperatures dropped to 35 °C (V-down), 33 °C (flat), and 32 °C (V-up), corresponding to the gradual decline in solar radiation in the afternoon and increased convective losses as the ambient temperature started to decrease.

Figure 8 presents the temperature profiles of the outlet air (T_{out}), absorber plate (T_{plate}), and glass cover (T_{glass}) for the three solar air heater designs, flat, V-down, and V-up, on 18 February 2025, under the lowest tested mass flow rate of 0.00882 kg/s.

At 09:00, the day began with cooler morning temperatures and moderate solar radiation (490 W/m^2). This early condition resulted in initial outlet air temperatures of about 24 °C (V-down), 21 °C (flat), and 21 °C (V-up). These values were noticeably higher than those recorded at the same hour on 15 February, primarily because the ambient temperature was significantly higher (27°C) and the low mass flow rate allowed longer residence time of air in the duct, thus enhancing heat gain. As the day progressed and solar radiation increased, reaching a peak of 1020 W/m^2 at around 12:30, the outlet temperatures began to climb steadily. By 13:00, peak values of 52 °C (V-down), 50 °C (V-up), and 48 °C (flat) were observed. Again, the V-down SAH demonstrated the highest outlet temperature, supported by enhanced internal turbulence and a more efficient heat transfer mechanism. Interestingly, although the solar radiation on this day was slightly lower than on 15 February, the outlet air temperatures were generally higher. This counterintuitive result is attributed to the lower mass flow rate, which in

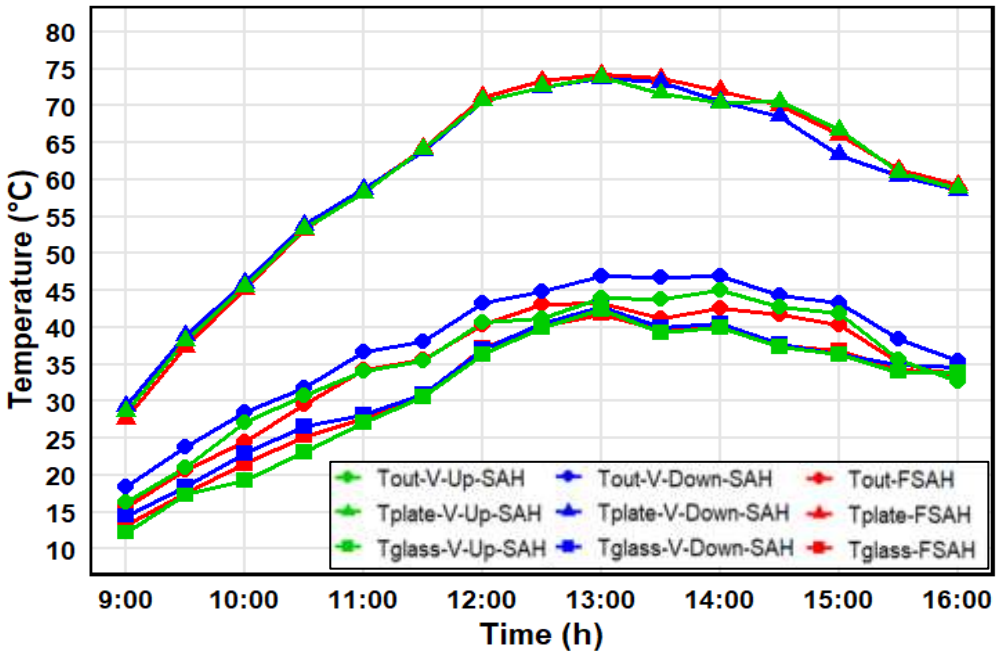

Fig. 7 Daily variation of temperatures for flat, V-up, and V-down solar air heaters on 15 – 02 –2025 at 0.01764 kg/s.

terms of absorber plate temperatures, peak values were recorded between 13:00 and 13:30. The flat SAH reached 78°C, slightly higher than the V-up (77°C) and V-down (76°C). This inversion, where the flat plate recorded the highest absorber plate temperature, is because it's less efficient at air movement, and because the flat duct has lower turbulence, it tends to retain more heat in the absorber, resulting in higher plate temperatures but less effective heat transfer to the air. The glass cover temperatures also followed a similar trend, peaking around 45°C (V-down) and 44°C for both flat and V-up SAHs. By 16:00, the outlet temperatures declined to 37°C (V-down), 36°C (flat), and 35°C (V-up), reflecting the reduction in solar intensity and a gradual cooling of the system components.

Figure 9. shows the variation of outlet air temperature (T_{out}), absorber plate temperature (T_{plate}), and glass cover temperature (T_{glass}) for the three types of solar air heaters, flat, V-down, and V-up, on 25 February 2025 at a moderate mass flow rate of 0.01323 kg/s.

At 09:00, the experiment began with a relatively lower ambient temperature (5°C), and solar radiation started at 530 W/m², similar to other test days. The initial outlet temperatures recorded were 12°C (V-down), 8°C (flat), and 10°C (V-up), with slight variations attributed to the morning solar input and system heat-up lag. As the sun rose and radiation increased, peaking around 1050 W/m² between 12:30 and 13:00, the outlet temperatures also rose. The V-down configuration once again outperformed the others, reaching a peak Tout of 39°C around 13:30, followed by 34°C (flat) and 35°C (V-up). Absorber plate temperatures reached their maximum values between 13:00 and 13:30, recorded at 71°C for V-down, 69°C for flat, and 68°C for V-up. These values are slightly lower than the outlet air temperatures and absorber temperatures on 18 February due to faster air movement inside the duct, which effectively carried heat away from the absorber, reducing its peak temperature.

Glass cover temperatures followed a similar trend, with peak values ranging between 33°C and 32°C, which is also lower than on the other days. By 16:00, as solar radiation dropped below 700 W/m² and ambient temperatures began to decline slightly, the outlet air temperatures decreased to about 27 °C (V-down), 26 °C (flat), and 27 °C (V-up). This decline was a direct result of the falling solar input and increased thermal losses during the later part of the day.

Figure 10. displays the variation in useful heat transfer rate (Q_{out}) for the three solar air heater configurations, flat, V-down, and V-up, on 15 February 2025, operating at the highest mass flow rate of 0.01764 kg/s.

At the start of the test at 09:00, solar radiation was around 520 W/m², and the ambient temperature was 9°C. Under these conditions, the useful heat output was 200 W for the flat SAH, 205 W for the V-up, and 240 W for the V-down SAH. As solar

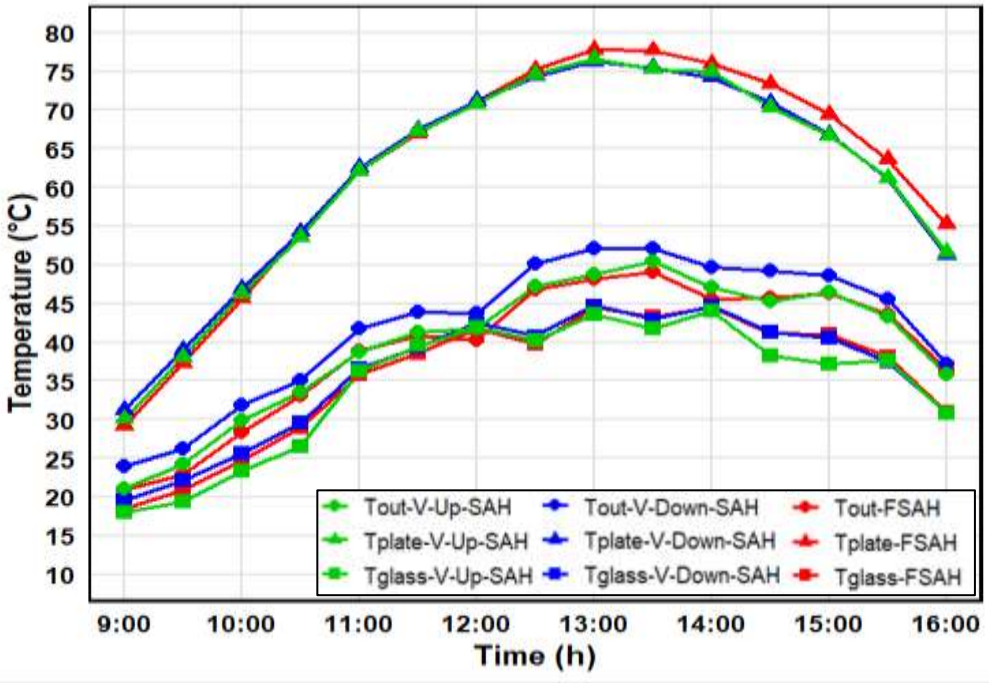

Fig. 8 Daily variation of temperatures for flat, V-up, and V-down solar air heaters on 18–02–2025 at 0.00882 kg/s.

radiation steadily rose and reached its peak value of $1040\ W/m^2$ at 12:30, and the ambient temperature increased to around 24 ℃ the heat transfer rates for all three collectors correspondingly increased.

The V-down SAH peaked at about 529 W, followed by the V-up at around 492 W, and the flat SAH at 470 W. These values reflect the strong influence of both high solar radiation and high mass flow rate, which allows more air to absorb heat per unit of time, even though the air does not remain in the duct for a long time. From around 13:30 onwards, as solar radiation began to decline (dropping below $900\ W/m^2$), the Q_{out} values also started to decrease. This decline continued throughout the afternoon, driven by falling solar radiation, a lower temperature difference between the absorber and air, and gradual thermal losses to the environment. By 16:00, the useful heat output had fallen to about 221 W (flat), 286 W (V-up), and 326 W (V-down). Despite having the highest mass flow rate among all test days, the V-down configuration consistently outperformed the others due to its aerodynamically optimized design. The perforated downward-facing ribs promote vortex formation and chaotic flow, increasing heat transfer area and effectiveness, especially under high flow conditions. The flat SAH, lacking internal roughness, showed the lowest Q_{out} throughout the day, confirming that the presence of artificial roughness is essential for enhancing thermal performance.

Figure 11. illustrates the variation in useful heat transfer rate (Q_{out}) for the flat, V-up, and V-down solar air heater (SAH) configurations on 18 February 2025, at the lowest tested mass flow rate of 0.00882 kg/s.

At 09:00, the solar radiation was around $490\ W/m^2$, and the ambient temperature was relatively high at about 15℃. Under these conditions, Q_{out} started at approximately 100 W for the flat SAH, 110 W for the V-up, and 130 W for the V-down SAH. As the day progressed, solar radiation rose to a peak of approximately $1020\ W/m^2$ between 12:30 and 13:00, while the ambient temperature reached its highest recorded value across all test days, at around 27 ℃. These conditions led to a noticeable increase in heat transfer. The V-down SAH reached its maximum Q_{out} of about 284 W, while the V-up SAH achieved approximately 260 W, and the flat SAH peaked near 236 W.

This performance boost was significantly influenced by two key factors: the lower mass flow rate, which allowed the air to stay longer inside the duct, increased the residence time, and enabled more heat absorption. The high ambient temperature reduced the temperature gradient between the glass and its surroundings, thereby minimizing heat losses through the cover. From around 13:30, Q_{out} values began to decline as solar radiation decreased due to the sun's angle shifting westward, possibly accompanied by slight cloud

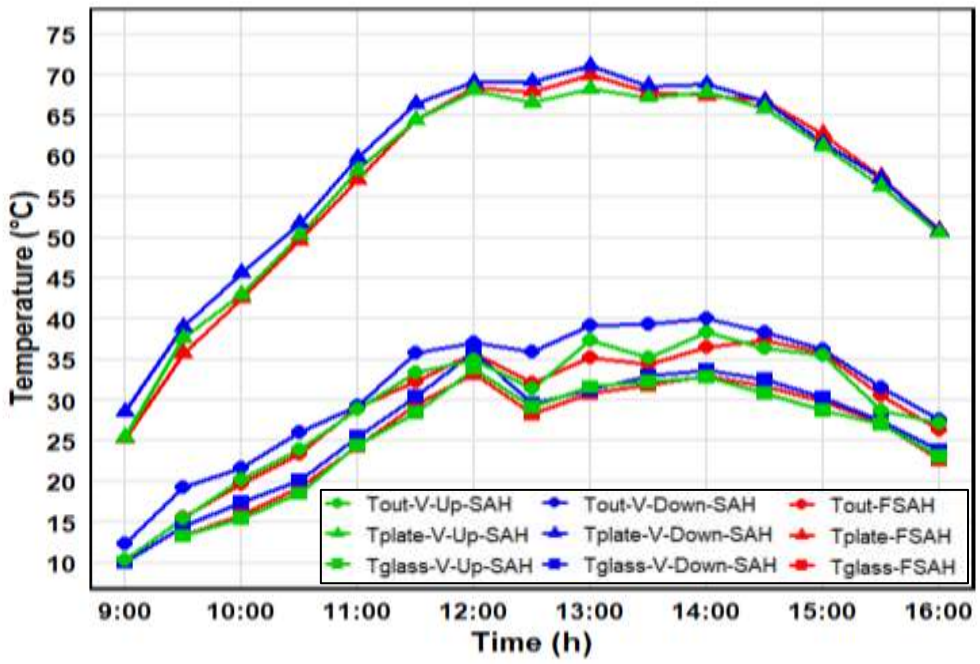

Fig.9 Daily variation of temperatures for flat, V-up, and V-down solar air heaters on 25–02–2025 at 0.01323 kg/s.

coverage around 14:00, which caused small fluctuations in irradiance. By 16:00, the heat output dropped to around 132 W (flat SAH), 140 W (V-up), and 156 W (V-down SAH).

It is worth noting that, although this day experienced the lowest solar radiation levels among the three test days, its thermal performance remained strong. This advantage is due to the beneficial effect of the low mass flow rate, which improves thermal energy transfer, and the warm ambient conditions, which together contribute to efficient energy capture. Throughout the day, the V-down configuration maintained superior heat transfer, proving that its perforated, downward-facing ribs provide consistent thermal enhancement.

Figure 12. presents the variation in useful heat transfer rate (Q_{out}) for the flat, V-up, and V-down solar air heater configurations on 25 February 2025, under a moderate mass flow rate of 0.01323 kg/s.

At the beginning of the experiment at 09:00, the recorded solar radiation was about 520 W/m^2, and the ambient temperature was 4°C, resulting in lower initial heat transfer. Q_{out} values started at about 110 W for the flat SAH, 124 W for the V-up SAH, and 157 W for the V-down SAH. As the day advanced, solar radiation rose significantly, reaching its peak at over 1050 W/m^2 around 12:30–13:00, making this the day with the highest solar radiation among all test days.

Ambient temperature also increased, peaking at 14.5°C, providing favorable conditions for heat transfer. Under these circumstances, the V-down SAH reached a maximum Q_{out} of 395 W, the V-up SAH peaked at 369 W, and the flat SAH reached 335 W.

Following the peak performance, Q_{out} values gradually declined starting around 13:30, as solar radiation began to drop due to the natural diurnal cycle. However, the decrease was not steep, indicating relatively stable weather conditions with minimal cloud interference during the afternoon. By 16:00, the useful heat output was about 165 W (flat SAH), 193 W (V-up SAH), and 200 W (V-down SAH).

The performance hierarchy remained consistent throughout the day, with the V-down configuration outperforming the others due to the enhanced turbulence, increased heat transfer surface area, and better flow disruption provided by the downward-facing perforated ribs. The V-up SAH followed, while the flat SAH lagged, confirming that smooth surfaces without artificial roughness are less effective in absorbing and transferring thermal energy, especially under moderate flow rates. To further validate these results, they were compared with previously reported studies on rib-roughened solar air heaters, Table 2 showing that the observed efficiencies and useful heat gains fall within the ranges reported in the literature, thereby confirming the reliability of the present experimental findings.

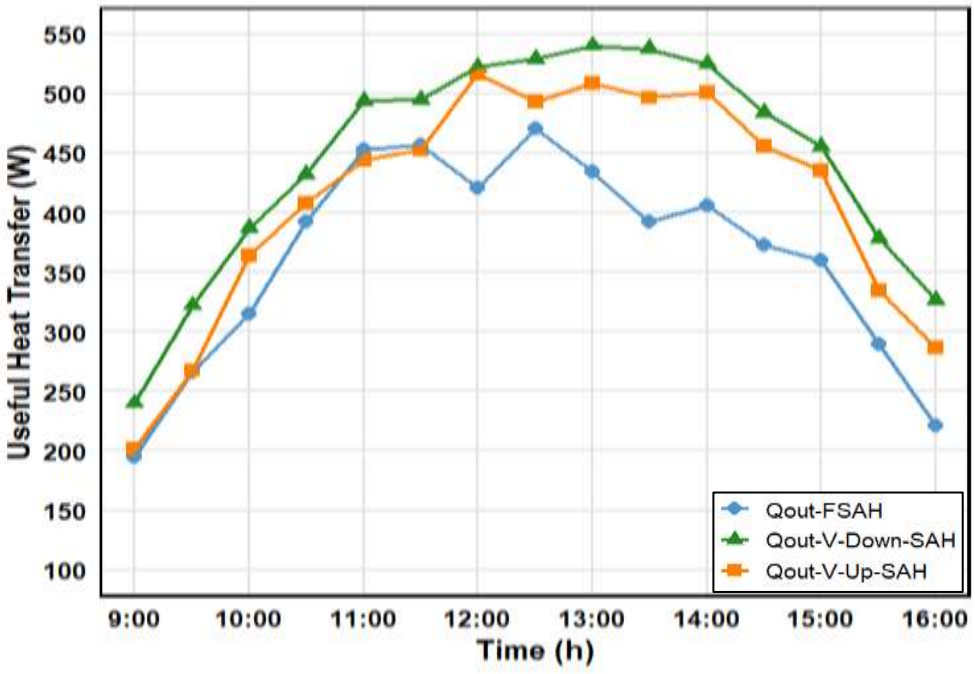

Fig. 10 Useful heat transfer variation for FSAH, V-up SAH, and V-down SAH on 15–02–2025 at 0.01764 kg/s.

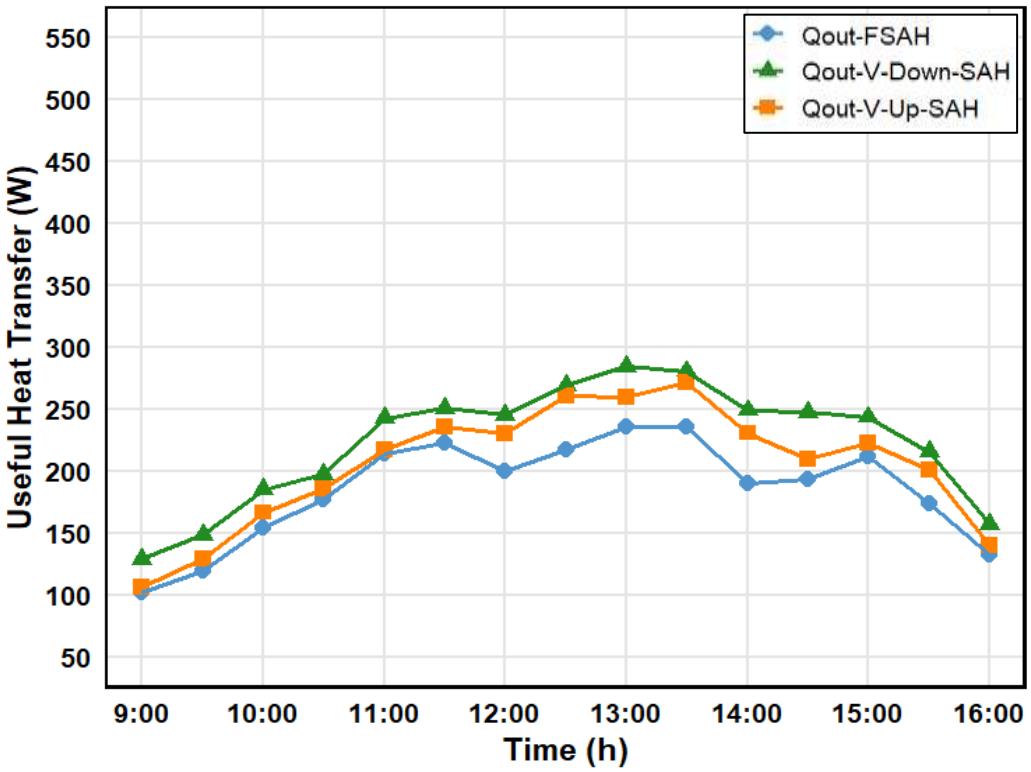

Fig. 11 Useful heat transfer variation for FSAH, V-up SAH, and V-down SAH on 18–02–2025 at 0.00882 kg/s.

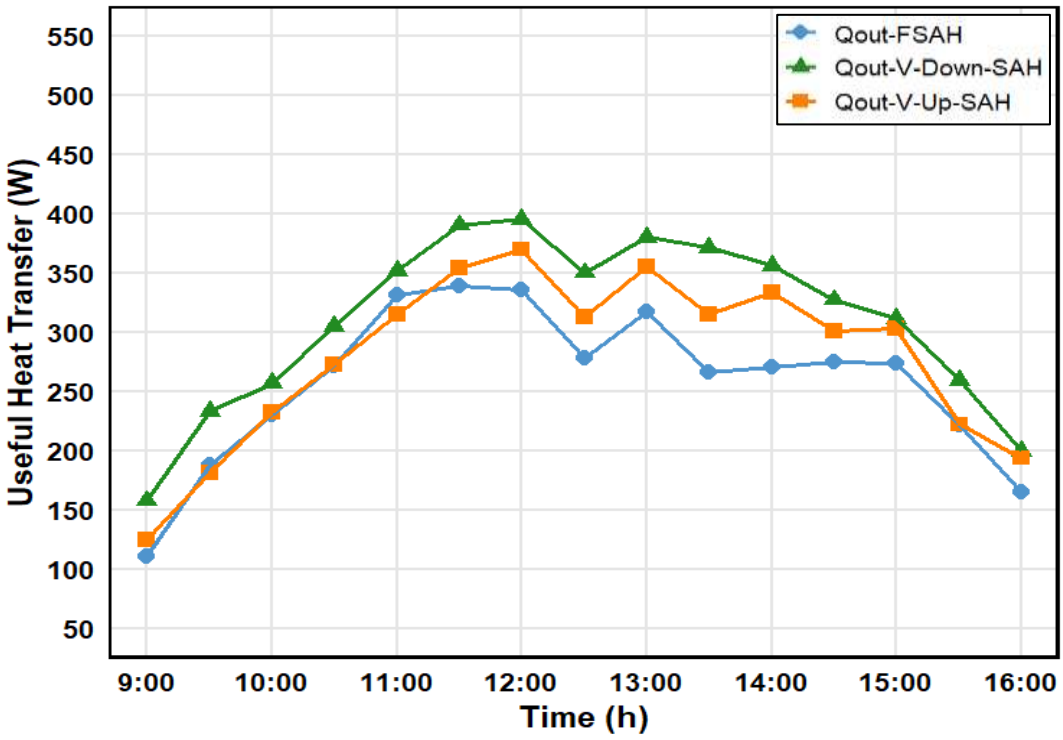

Fig. 12 Useful heat transfer variation for FSAH, V-up SAH, and V-down SAH on 25–02–2025 at 0.01323 kg/s.

Table 2. Validation of the present study with reported literature

References	Type of Rib	Optimized Parameters	Key Findings
Momin et al. [22]	V-shaped ribs	e/Dh = 0.02 – 0.034, α = 60°	Nusselt number rose 2.30 times and friction factor 2.83 times over the smooth duct
Hans et al. [6]	Multi-V ribs	e/Dh = 0.019 – 0.043, P/e = 6–12, W/w = 6	Peak Nusselt number and friction factor occurred at α = 60°, with heat transfer increasing up to about six times
Singh et al. [8]	Discrete V-down ribs	P/e = 8, g/e = 1 d/w = 0.65, α = 60° e/Dh = 0.043	Effective efficiency reached up to about 91%, with higher pumping power
Singh et al. [9]	V-down ribs with a gap	e/Dh = 0.043, P/e = 8 α = 60°	Performance parameter g = 2.06 at Re = 12000
Patel & Lanjewar [13]	Staggered discrete V ribs	e/Dh = 0.045, P/e = 12 α = 60°	Optimum thermal efficiency = 86%
Jain et al. [14]	Multi-gap V ribs with staggered elements	P/e = 12, w/g = 1 (r/e) = 3.5	Thermal efficiency increased from 42% to 87%
Present study	Multi-V perforated ribs (V-up, V-down, flat)	W/w = 5, P/e = 10 e/Dh = 0.06, AR = 5	Maximum daily efficiency was 84% for V-down, 77% for V-up, and 69% for flat, while peak useful heat gain reached 529 W, 492 W, and 470 W, respectively.

5. UNCERTAINTY ANALYSIS

To ensure the accuracy and credibility of the experimental results, an uncertainty analysis was conducted in accordance with the methodology described by Holman 2021. [23] using the root sum square (RSS) approach. This analysis evaluates the propagation of uncertainties through the key calculated parameters, namely: the useful heat gain Q_u , thermal efficiency η. The uncertainty of observed and calculated data for F-SAH, V-Down SAH, and V-Up SAH is shown in Table 3, The general propagation of uncertainty for a function of multiple variables is given by:

$$\frac{\Delta R}{R} = \sqrt{\left(\frac{\partial R}{\partial x_1} * \frac{\Delta x_1}{R}\right)^2 + \left(\frac{\partial R}{\partial x_2} * \frac{\Delta x_2}{R}\right)^2 + \cdots} \quad (4)$$

Where:

- R is the derived quantity.
- x_1, x_2,… are the measured variables.
- ∂x_1, ∂x_2,… are the uncertainties of these variables.

1. Useful Heat Gain Q_u:

$$Q_u = \dot{m} \times Cp \times \Delta T \quad (5)$$

The uncertainty in Q_u :

$$\frac{\Delta Q_u}{Q_u} = \sqrt{\left(\frac{\Delta \dot{m}}{\dot{m}}\right)^2 + \left(\frac{\Delta Cp}{Cp}\right)^2 + \left(\frac{\Delta(\Delta T)}{\Delta T}\right)^2} \quad (6)$$

2. Thermal Efficiency η_{th} :

$$\eta_{th} = Q_u / (A_c \times I) \quad (7)$$

Uncertainty in η_{th} :

$$\frac{\Delta \eta_{th}}{\eta_{th}} = \sqrt{\left(\frac{\Delta Q_u}{Q_u}\right)^2 + \left(\frac{\Delta I}{I}\right)^2 + \left(\frac{\Delta(A)}{A}\right)^2} \quad (8)$$

Table 3: Summary of calculated data and uncertainty analysis results.

Date	SAH Type	Q_u (w)	η_{th} (%)	ΔQ_u (w)	$\Delta\eta_{th}$ (%)
16-02-2025	F-SAH	105.75	36.56	± 4.55	± 1.57
16-02-2025	V-Down SAH	125.47	43.38	± 4.60	± 1.58
16-02-2025	V-Up SAH	122.41	42.32	± 4.59	± 1.58
25-02-2025	F-SAH	165.35	46.89	± 6.84	± 1.94
25-02-2025	V-Down SAH	199.44	56.56	± 6.94	± 1.96
25-02-2025	V-Up SAH	193.59	54.90	± 6.92	± 1.95

5. CONCLUSION

This experimental study evaluated the thermal performance of three solar air heater (SAH) configurations: flat plate, V-down perforated, and V-up perforated absorber plates under real outdoor conditions at the University of Zakho, Zakho, Iraq, during February 2025. Tests were performed at three different mass flow rates:

0.00882 kg/s, 0.01323 kg/s, and 0.01764 kg/s, with temperature and radiation data recorded at 30-minute intervals.

The results revealed that the V-down perforated SAH consistently delivered superior performance. At the highest tested flow rate (0.01764 kg/s), it achieved a maximum daily thermal efficiency of 84%, compared to 77% for the V-up and 69% for the flat plate. Corresponding useful heat transfer rates were approximately 529 W (V-down), 492 W (V-up), and 470 W (flat plate).

At the moderate flow rate (0.01323 kg/s), the daily efficiencies were 56% (V-down), 50% (V-up), and 47% (flat plate), while corresponding useful heat transfer peaks reached 395 W, 369 W, and 335 W, respectively. At the lowest flow rate (0.00882 kg/s), efficiencies decreased to 43% (V-down), 39% (V-up), and 36% (flat), with maximum useful heat transfer values of 284 W (V-down), 260 W (V-up), and 236 W (flat), respectively.

These improvements were primarily due to the enhanced turbulence and improved heat transfer enabled by the V-down perforated ribs. This configuration enabled more effective air surface contact, resulting in higher outlet temperatures and increased heat extraction across all test conditions.

To summarize, this study confirms that the V-down configuration offers the best thermal performance among the tested designs. More importantly, the results validate that rib-roughened absorbers can achieve high efficiency under Iraqi climatic conditions, reinforcing findings reported in earlier literature. The tested designs rely on simple, low-cost fabrication techniques, making them particularly attractive for resource-limited settings where affordable solar heating is essential. Rather than claiming a breakthrough, this work provides a practical experimental benchmark that demonstrates the effectiveness of rib orientation and perforation as reliable performance-enhancement strategies for solar air heaters.

Greek Symbols

η_{th}	Thermal efficiency, %
α	Angle of attack of ribs, degrees (°)
ρ	Air density, kg/m^3

Nomenclature

T_{in}	Air inlet temperature, ℃
T_{out}	Air outlet temperature, ℃
T_{plate}	Absorber plate temperature, ℃
T_{glass}	Glass cover temperature, ℃
T_{amb}	Ambient temperature, ℃
I	Solar radiation intensity, W/m^2
A_S	Collector surface area, m^2
$\dot{m}$	Air mass flow rate, kg/s
Cp	Specific heat of air, $J/kg \cdot K$
Q_U	Useful heat gain, W
E	Rib height, m
P	Pitch between ribs, m
A_C	Cross sectional area of duct, m^2
L	Duct length, m
H	Duct height, m
A/R	Duct aspect ratio
e/D_h	Relative roughness height
P/e	Relative roughness pitch
W/w	Relative rib width ratio
D_h	Hydraulic diameter, m
H	Duct height, m

Abbreviation

SAH	Solar Air Heater
FSAH	Flat Plate Solar Air Heater
V-down SAH	V-down Perforated Rib Solar Air Heater
V-up SAH	V-up Perforated Rib Solar Air Heater
SD card	Secure Digital Card
RTC	Real-Time Clock
UNO	Arduino Uno Microcontroller
DS18B20	Digital Temperature Sensor

REFERENCES

[1] F. Bayrak, H. F. Oztop, and A. Hepbasli, "Energy and exergy analyses of porous baffles inserted solar air heaters for building applications," *Energy Build.*, vol. 57, no. February, pp. 338–345, 2013, doi: 10.1016/j.enbuild.2012.10.055.

[2] R. Pandey, M. Kumar, and J. S. Saini, "Experimental study of parametric influence on heat transfer and friction in a rectangular duct having V-down baffle blocks with staggered racetrack-shaped openings," *Exp. Heat Transf.*, vol. 35, no. 6, pp. 818–847, 2022, doi: 10.1080/08916152.2021.1951898.

[3] J. A. Duffie, W. A. Beckman, and N. Blair, *Solar engineering of thermal processes, photovoltaics and wind*, 5th editio. Canada:

John Wiley & Sons, 2020.

[4] S. K. Sharma and V. R. Kalamkar, "Thermo-hydraulic performance analysis of solar air heaters having artificial roughness–A review," *Renew. Sustain. Energy Rev.*, vol. 41, pp. 413–435, 2015, doi: 10.1016/j.rser.2014.08.051.

[5] A.-M. E. Momin, J. S. Saini, and S. C. Solanki, "Heat transfer and friction in solar air heater duct with V-shaped rib roughness on absorber plate," *Int. J. Heat Mass Transf.*, vol. 45, no. 16, pp. 3383–3396, 2002, doi: 10.1016/S0017-9310(02)00046-7.

[6] V. S. Hans, R. P. Saini, and J. S. Saini, "Heat transfer and friction factor correlations for a solar air heater duct roughened artificially with multiple v-ribs," *Sol. energy*, vol. 84, no. 6, pp. 898–911, 2010, doi: 10.1016/j.solener.2010.02.004.

[7] S. Singh, S. Chander, and J. S. Saini, "Heat transfer and friction factor of discrete V-down rib roughened solar air heater ducts," *J. Renew. Sustain. Energy*, vol. 3, no. 1, pp. 1–18, 2011, doi: 10.1063/1.3558865.

[8] S. Singh, S. Chander, and J. S. Saini, "Thermal and effective efficiency based analysis of discrete V-down rib-roughened solar air heaters," *J. Renew. Sustain. Energy*, vol. 3, no. 2, 2011, doi: 10.1063/1.3574430.

[9] S. Singh, S. Chander, and J. S. Saini, "Investigations on thermo-hydraulic performance due to flow-attack-angle in V-down rib with gap in a rectangular duct of solar air heater," *Appl. Energy*, vol. 97, pp. 907–912, 2012, doi: 10.1016/j.apenergy.2011.11.090.

[10] R. Karwa and G. Chitoshiya, "Performance study of solar air heater having v-down discrete ribs on absorber plate," *Energy*, vol. 55, pp. 939–955, 2013, doi: 10.1016/j.energy.2013.03.068.

[11] S. Singh, S. Chander, and J. S. Saini, "Thermo-hydraulic performance due to relative roughness pitch in V-down rib with gap in solar air heater duct—comparison with similar rib roughness geometries," *Renew. Sustain. Energy Rev.*, vol. 43, pp. 1159–1166, 2015, doi: 10.1016/j.rser.2014.11.087.

[12] T. Istanto, D. Danardono, I. Yaningsih, and A. T. Wijayanta, "Experimental study of heat transfer enhancement in solar air heater with different angle of attack of V-down continuous ribs," in *AIP conference proceedings*, AIP Publishing LLC, 2016, p. 60002. doi: 10.1063/1.4949309.

[13] S. S. Patel and A. Lanjewar, "Experimental investigation of solar air heater duct with discrete V-rib integrated with staggered elements," *Int. J. Sustain. Eng.*, vol. 14, no. 2, pp. 162–171, 2021, doi: 10.1080/19397038.2020.1737752.

[14] P. K. Jain, A. Lanjewar, R. Jain, and K. B. Rana, "Performance analysis of multi-gap V-roughness with staggered elements of solar air heater based on artificial neural network and experimental investigations," *Environ. Sci. Pollut. Res.*, vol. 28, no. 25, pp. 32905–32920, 2021, doi: 10.1007/s11356-021-12875-0.

[15] V. K. Balakrishnan, M. Gurunathan, R. K. Parthasarathy, and V. R. Poluru, "Experimental analysis of solar air heater using polygonal ribs in absorber plate integrated with phase change material," *Therm. Sci.*, vol. 26, no. 4 Part A, pp. 3187–3199, 2022, doi: 10.2298/TSCI210518345V.

[16] L. T. Zubairi, M. Danismaz, N. J. Yasin, and W. A. M. Al-Shohani, "Comparative Analysis of Thermal Performance in Dual-Flow Solar Air Heaters Utilizing Diverse Absorber Plates.," *Int. J. Heat Technol.*, vol. 41, no. 4, 2023, doi: 10.18280/ijht.410423.

[17] V. Rajendran *et al.*, "Enhancing the performance of a solar air heater by employing the broken V-shaped ribs," *Environ. Sci. Pollut. Res.*, vol. 30, no. 31, pp. 77807–77818, 2023, doi: 10.1007/s11356-023-27814-4.

[18] T. L. Bergman, *Fundamentals of heat and mass transfer*, 7th editio. John Wiley & Sons, 2011. [Online]. Available: https://books.google.com/books?id=vvyIoXEywMoC

[19] J. A. Duffie and W. A. Beckman, *Solar engineering of thermal processes*, Fourth Edi. Canada: John Wiley & Sons, 2013. [Online]. Available: https://www.sku.ac.ir/Datafiles/BookLibrary/45/John A. Duffie, William A. Beckman(auth.)-Solar Engineering of Thermal Processes, Fourth Edition (2013).pdf

[20] A. Mermoud, "PVSyst–Logiciel Photovoltaïque," *ISE, Univ. Geneva*, 2012, [Online]. Available: https://www.pvsyst.com/.

[21] D. H. Rhee, D. H. Lee, H. H. Cho, and H. K. Moon, "Effects of duct aspect ratios on heat/mass transfer with discrete V-shaped ribs," *Turbo Expo Power Land, Sea, Air*, vol. 36886, pp. 509–516, 2003, doi: 10.1115/GT2003-3862.

[22] A.-M. E. Momin, J. S. Saini, and S. C. Solanki, "Heat transfer and friction in solar air heater duct with V-shaped rib roughness on absorber plate," *Int. J. Heat Mass Transf.*, vol. 45, no. 16, pp. 3383–3396, 2002, doi: 10.1016/j.energy.2011.03.054.

[23] J. P. Holman, *ExperimentalMethods forEngineers*, 8th editio. New York, 2012. [Online]. Available: https://mech.at.ua/HolmanICS.pdf